HHS Public Access

Author manuscript

Vaccine. Author manuscript; available in PMC 2018 April 25.

Published in final edited form as:

Vaccine. 2017 April 25; 35(18): 2404–2412. doi:10.1016/j.vaccine.2017.03.036.

Semiconductor diode laser device adjuvanting intradermal vaccine

Yoshifumi Kimizuka, MD, PhD[1], **John J. Callahan, PhD**[2], **Zilong Huang, MS**[2,3], **Kaitlyn Morse, PhD**[1], **Wataru Katagiri, BS**[4], **Ayako Shigeta, MD**[1], **Roderick Bronson, PhD**[5], **Shu Takeuchi**[1], **Yusuke Shimaoka**[1], **Megan P. K. Chan, BS**[1], **Yang Zeng, MD, PhD**[1], **Binghao Li, MD**[1], **Huabiao Chen, MD**[1], **Rhea Y. Y. Tan, BS**[1], **Conor Dwyer**[1], **Tyler Mulley, BS**[2], **Pierre Leblanc, PhD**[1], **Calum Goudie, MD**[1], **Jeffrey Gelfand, MD**[1], **Kosuke Tsukada, PhD**[4], **Timothy Brauns, MBA**[1], **Mark C. Poznansky, MD PhD**[1], **David Bean, MS**[2,3,#], and **Satoshi Kashiwagi, MD, PhD**[1,#]

[1]Vaccine and Immunotherapy Center, Division of Infectious Diseases, Department of Medicine, Massachusetts General Hospital, 149 13th Street, Charlestown, Massachusetts, 02129, United States of America

[2]SemiNex Corporation, 100 Corporate Place, Suite 401, Peabody, Massachusetts, 01960, United States of America

[3]Veralase LLC, 135 East Street, Middleton, Massachusetts, 01949, United States of America

[4]Graduate School of Fundamental Science and Technology, Keio University, 3-14-1 Hiyoshi, Kohoku-ku, Yokohama, Kanagawa 223-8522, Japan

[5]Department of Pathology, Harvard Medical School, 77 Avenue Louis Pasteur, Boston, Massachusetts 02115, United States of America

Abstract

[#]**Correspondence should be addressed:** Satoshi Kashiwagi, MD, PhD, Assistant Professor of Medicine, Vaccine and Immunotherapy Center, Division of Infectious Diseases, Department of Medicine, Massachusetts General Hospital, Harvard Medical School, 149 13th Street, Charlestown, Massachusetts, 02129, Tel: 617-726-6265, Fax: 617 726 5411, skashiwagi@mgh.harvard.edu; or David Bean, MS, Chief Executive Officer, Veralase LLC, 135 East Street, Middleton, Massachusetts, 01949, Tel: 978-273-3562, dbean@veralase.com.

Author contributions: Y Kimizuka performed most of the experiments; JJ Callahan, Z Huang, T Mulley, D Bean designed and manufactured the handheld laser devices; Y Kimizuka, K Morse, B Li, Z Yang, H Chen, Y Shimaoka, S Takeuchi, S Kashiwagi performed vaccination study; S Takeuchi, Y Shimaoka, M Chan, C Dwyer, Y Kimizuka, A Shigeta, RYY Tan, P Leblanc, C Goudie performed immunoassays; Y Kimizuka, JJ Callahan, S Kashiwagi designed the experiments; R Bronson, Y Kimizuka, A Shigeta, K Tsukada, W Katagiri performed skin damage study; Y Kimizuka, JJ Callahan, R Bronson, K Tsukada, W Katagiri, S Kashiwagi analyzed the data; T Brauns, J Gelfand, D Bean, JJ Callahan, S Kashiwagi designed the study; M Poznansky, JJ Callahan, D Bean, S Kashiwagi wrote the manuscript.

Potential conflict of interest:

David Bean is Chief Executive Officer of Veralase LLC and receives salary support and holds equity from Veralase LLC. John Callahan is Vice President of Engineering at SemiNex Corporation and receives salary support and holds equity from SemiNex Corporation. Zilong Huang is an employee of Veralase LLC and receives salary support from Veralase LLC. Tyler Mulley is an employee of SemiNex Corporation and receives salary support from SemiNex Corporation. These do not alter the authors' adherence to Vaccine's policies on sharing data and materials.

A brief exposure of skin to a low-power, non-tissue damaging laser light has been demonstrated to augment immune responses to intradermal vaccination. Both preclinical and clinical studies show that this approach is simple, effective, safe and well tolerated compared to standard chemical or biological adjuvants. Until now, these laser exposures have been performed using a diode-pumped solid-state laser (DPSSL) devices, which are expensive and require labor-intensive maintenance and special training. Development of an inexpensive, easy-to-use and small device would form an important step in translating this technology toward clinical application

Here we report that we have established a handheld, near-infrared (NIR) laser device using semiconductor diodes emitting either 1061, 1258, or 1301 nm light that costs less than $4,000, and that this device replicates the adjuvant effect of a DPSSL system in a mouse model of influenza vaccination. Our results also indicate that a broader range of NIR laser wavelengths possess the ability to enhance vaccine immune responses, allowing engineering options for the device design.

This small, low-cost device establishes the feasibility of using a laser adjuvant approach for mass-vaccination programs in a clinical setting, opens the door for broader testing of this technology with a variety of vaccines and forms the foundation for development of devices ready for use in the clinic.

Keywords

laser; semiconductor laser diode; near-infrared; handheld; adjuvant; vaccine

Introduction

In recognition of the clear advantages of skin-based vaccination [1–3], a growing range of technologies are now in use or at an exploratory stage of their development for intradermal delivery of vaccine antigen [4, 5]. For the maximum efficacy, the intradermal vaccination strategy would further benefit from use of adjuvants to reduce antigen dose or the number of vaccinations used in order to generate protective immunity [5–8]. However, development of adjuvants for intradermal vaccines is especially challenging, as most conventional adjuvants are likely to be inappropriate for use in the skin due to issues related to viscosity, formulation with antigen, or the potential to induce persistent local inflammation [9, 10]. There is clearly a need for new adjuvants that are compatible with intradermal vaccination.

A physical parameter such as laser light may serve as an alternative to conventional chemical or biological adjuvants [11, 12]. Brief exposures of a small area of the skin to non-tissue damaging high-power, nanosecond pulses of visible light lasers before intradermal vaccination has been shown to increase immune responses to a clinically relevant vaccine in mice and humans [10, 12–14]. However, these initial approaches are constrained by a key barrier; production of such a pulsed laser requires large devices that cannot easily be reduced to small and economical form factors. We have recently demonstrated the ability of short duration treatment with low-power, non-pulsed, 1064 nm lasers to augment immune responses to intradermal vaccine in a lethal challenge murine influenza model [15]. In contrast to the complicated technical requirements for visible pulsed lasers, elimination of

the need for high-power pulses on continuous wave (CW) 1064 nm near-infrared (NIR) laser makes it feasible to produce relatively small and inexpensive laser devices.

In spite of the obvious advantages to utilizing such small CW NIR laser devices, appropriate devices are not currently being produced for medical applications. This device development gap forms an obstacle to further translation of the laser vaccine adjuvant approach into human studies. Here we report that we successfully developed a handheld NIR laser device for adjuvanting vaccines that can be made at a substantially lower cost than current commercially-available systems. Showing that the same laser adjuvanting effects can be produced by lasers based on inexpensive diodes as are produced by more expensive diode-pumped solid-state lasers (DPSSLs) addresses one of the practical limitations of using NIR lasers in a clinical setting.

Materials and Methods

Design and assembly of a handheld NIR laser device

SemiNex Corporation (Peabody, MA) incorporated a Gallium arsenide (GaAs) 1061 nm semiconductor laser diode from Axcel Photonics (Marlborough, MA) or Indium phosphide (InP) 1258 semiconductor laser diode from Innolume (Dortmund, Germany) or 1301 nm semiconductor laser diode from SemiNex into the SemiNex Laser Engine platform, which had previously developed for consumer market applications at a different wavelength [16]. The details are described in the Supplementary Materials and Methods.

Measurement of the spot size of a handheld NIR laser device

To measure the spot size of the device, an infrared (IR) camera (Sensors Unlimited, Princeton NJ) was used, as the emitted light is not visible to the naked eye. The IR camera consisted of an array of pixels which would translate the IR light into a color image on a computer screen. The details of the measurement are described in the Supplementary Materials and Methods.

Measurement of the wavelength profile of a handheld NIR laser device

To measure the wavelength emitted from the device, an Aniritsu MS9710B Optical Spectrum Analyzer (OSA) was used. The reported emission wavelength from a laser diode is the nominal center wavelength. However, laser diodes emit within a distribution of wavelengths around the center wavelength. Average output powers were determined using a power meter for each illumination (Thorlabs).

Control software design of a handheld NIR laser device

A control board of a handheld laser device was modified to accommodate greater operational flexibility within the R&D environment so researchers could modify the laser parameters such as power level, pulse width, duty cycle, and overall energy profile within the target tissue. The control board used an industry-standard wireless Bluetooth communication protocol and USB hardware connection to connect the laser to a PC for programming via a web interface. A web-based user interface was designed for programming the handheld units and monitoring the testing progress. The software was

hosted on a Microsoft 2012 Server platform running Microsoft SQL Server 2012. Data was communicated over the Internet using PHP protocol to a PC client that connected to the handheld laser device via USB.

Determination of skin thermal responses to handheld NIR laser

The maximum non-tissue damaging dosages for the handheld device were tested in mice as previously described [15] (see Supplementary Materials and Methods). Briefly, the handheld laser device was applied to the shaved and depilated backs of eight-week-old female C57BL/6J mice (stock no:000664 from Jackson Laboratory, ME) over a range of powers using three-minute exposures, with skin temperatures monitored using an infrared thermal imaging camera (FLIR Systems, North Billerica, MA) and assessment for skin damage using visible inspection and histology. All animal procedures were performed following the Public Health Service Policy on Humane Care of Laboratory Animals and approved by the Institutional Animal Care and Use Committee of Massachusetts General Hospital.

Mouse model of intradermal influenza vaccination

In order to examine the efficacy of the handheld laser as a vaccine adjuvant, we compared the handheld lasers to a previously explored DPSSL, (1064 nm neodymium-doped yttrium orthvanadate [Nd:YVO_4] laser) (RMI Laser, Lafayette CO), using an established mouse model of influenza vaccination as previously described [15]. Briefly, two days before the laser treatment, mice were depilated using a hair remover (Nair, Church & Dwight). Immediately after the completion of the laser treatment, mice were then injected intradermally with whole inactivated influenza virus A/PR/8/34 (H1N1) (1 μg in 10 μl saline, 1 spot, Charles River). Blood samples were taken 28 days after immunization and at 4 days post-challenge with an intranasal application of homologous live influenza virus (2×10^5 50% egg infectious doses per mouse, which is equivalent to 20 × 50% mouse lethal dose (MLD_{50}), in 30 μl saline 28 days after vaccination. A part of mice was monitored for body weight and survival time for 14 days post-challenge to assess protection. The details of the treatment are available in the Supplementary Materials and Methods.

ELISAs for quantitating anti-influenza antibodies

We assessed anti-influenza IgG and its subclasses and IgE antibody responses in serially diluted mouse serum samples by using ELISA, as previously described [15, 17] (see Supplementary Materials and Methods).

Hemagglutination inhibition (HAI) titration

Mouse sera were analyzed for hemagglutination inhibition (HAI) titers by SRI International (see Supplementary Materials and Methods).

Quantitation of T-cell response to influenza vaccination

For assessment of T cell responses after influenza challenge, we isolated splenoctyes 4 days post live influenza challenge as previously described [15]. Each splenocyte preparation was divided into 1×10^6 cells per 96-wells in duplicate and incubated with or without 10 μg/ml of influenza A peptides NP311 (MHC Class II, $NP_{311–325}$ QVYSLIRPNENPAHK,

Anaspec) or 10 μg/ml PA224 (MHC class I, $PA_{224–233}$ SSLENFRAYV) for 60 hours. IFN-γ or IL-4 amounts within supernatants (pg/ml) were determined using DuoSet ELISA kits (R&D Systems) following manufacturer's instructions.

Statistical analysis

For the analysis of serum antibody response, a log transformation of antibody titers was applied in order to reduce positive skewing in the distribution of the raw antibody titers which would violate parametric test assumptions. We used the Student's T-test for the comparison of numerical values between 2 groups, and the one-way ANOVA followed by the Tukey's honestly significant difference (HSD) tests for comparisons of more than three groups for all statistical analyses unless otherwise specified.

Results

Dimensions of handheld NIR laser device

We constructed three laser diode-based devices for adjuvanting vaccines. The 1061 nm device uses a GaAs semiconductor laser diode, while the 1258 or 1301 nm devices incorporated InP. The housing contained the laser engine, control board, rechargeable battery, USB interface and remote operation connection (Figure 1a). The handheld device was approximately 150 mm in length and was designed to fit with a hand with the top "fire" or "trigger" button located in the thumb position (Figure 1b). All of the handheld devices—1061 nm, 1258 nm and 1301 nm— had the same hardware and software builds.

A prototype handheld laser replicates the beam parameters of a larger DPSSL system

The spot size in the previous studies was mostly round in shape, and ranges from 0.2 to 0.4 cm^2 [10–12, 14, 15]. The handheld laser devices produced a rectangle target of 0.25 cm^2 rather than a round spot. Due to the generation of internal heat in a laser diode, the horizontal width of the spot of the devices was affected by the chosen operating power. To create the desired spot size, a standoff or "nosecone" was added to the final assembly to ensure the spot size was always consistent throughout the experiments (Supplementary Table 1).

In order to examine the beam profile, the IR images of handheld lasers were taken (Figure 2a–e). A number of peaks appeared within the Gaussian envelope due to the laser diode being able to support a number of different lasing modes. This was different from a solid-state or fiber laser which typically has only one lasing mode. The power distribution seen as the white lines across the horizontal section of the spot was relatively flat along the peak region, with a number of peaks and valleys which tapered off at the edge. The power distribution in the vertical direction has more of the Gaussian shape with a strong peak in the center and smaller peaks on either side. During operation, the peaks shifted within the distribution as the device was turned on and off.

The output power closely matched to the desired power setting within ± 5% error range (Figure 2f–h). The power range of the devices was 0–1.6, 0–1.7 and 0–2.0 W for the 1301

nm, 1258 nm and 1061 nm lasers respectively over an exposure area of 0.25 cm^2, with a maximum irradiance of 6–8 W/cm^2, which was deemed sufficient for laser adjuvanticity.

We were therefore able to replicate the emitted wavelength, beam profile, and irradiance of the previously explored DPSSL system, resulting in identical emitted doses.

Minimal wavelength shift observed for the handheld NIR laser device

Semiconductor laser diodes experience wavelength drift with temperature due to the internal chip heating with high current and high duty cycle in a predictable and linear manner. The InP diodes typically show a drift of 0.6 nm/°C for wavelengths between 1300 and 1700 nm. Diodes using GaAs materials at wavelengths between 780 nm and 1064 nm show a shift of 0.3 nm/°C. In order to establish the action spectrum of the immunostimulatory effect of the NIR laser adjuvant, the wavelength of the handheld lasers was measured in 0.2 nm steps and the power is reported in arbitrary units of milli-decibels (Figure 3). With the power range of the devices at 0–0.48, 0–0.5 and 0–1.25 W for the 1301 nm, 1258 nm and 1061 nm lasers respectively, wavelength shift observed was 2.0, 2.8, 2.8 nm at maximum. We therefore concluded that the effect of wavelength drift by heat generation was negligible in our system.

Delineation of non-tissue damaging dosages of handheld NIR laser parameters

We next determined the maximum non-tissue damaging dosages for the handheld NIR laser device. Maximum safe irradiances for the handheld NIR lasers were determined to be those at which skin temperatures did not exceed 43 °C and for which no visible or microscopic skin damage was detected [15]. We identified 5.0 W/cm^2 as the maximum safe irradiance for the 1061 nm laser (Figure 4a, left), 2.0 W/cm^2 for the 1258 nm laser (Figure 4a, middle), and 1.9 W/cm^2 for the 1301 nm laser (Figure 4a, right). Importantly, the thermal response of the 1061 nm laser (Figure 4a) showed good correspondence with that of CW 1064 nm DPSSL over a range of different irradiances [15]. At the maximum safe irradiances, no visible skin damage (Figure 4b) and no inflammatory response at any given time point (Figure 4c–d) was detected in any handheld laser-treated group. Thus, we concluded that the dosages of the handheld lasers below the maximum safe irradiance were non-tissue damaging.

The handheld NIR laser adjuvant enhances immune responses to intradermal vaccination without inducing an IgE response

Next, we examined the adjuvant effect of the handheld NIR lasers in an established murine influenza vaccination and lethal challenge model [15]. We compared the results from these lasers with that of the previously explored CW 1064 nm DPSSL [15], and a conventional chemical adjuvant, alum. In order to examine dose response, we also tested 50% of maximum safety dose for both 1258 and 1301 nm handheld NIR laser devices. The 1061, 1258 (low and high dose), 1301 (low dose) as well as CW 1064 nm DPSSL augmented pre-challenge IgG and IgG1 titers compared to the non-adjuvanted group, although the difference is not statistically significant (Supplementary Figure 1). Post-challenge, the 1061 nm ($P = 0.0131$), 1258 nm high ($P = 0.0009$) and low ($P = 0.0265$) dose, 1301 nm low dose ($P = 0.0003$), and alum ($P = 0.0477$) significantly augmented anti-influenza IgG titers

compared to the non-adjuvanted group (Figure 5a). In comparison, the CW 1064 nm DPSSL similarly augmented IgG (Figure 5a, $P = 0.0015$), and alum increased IgG1 titers (Figure 5b, $P < 0.0001$) with a significantly low IgG2c/IgG1 ratio (Figure 5e, $P < 0.0001$) and high anti-influenza specific IgE titers (Figure 5f, $P < 0.0001$) compared to non-adjuvanted control group. Importantly, the laser adjuvants did not change IgG2c/IgG1 ratio or increase IgE responses to the vaccine, which may be linked to subsequent hypersensitivity [18, 19] (Figure 5e–f).

Our previous study showed that CW 1064 nm DPSSL augments an effector $CD4^+$ T-cell response [15]. To determine the effect of the handheld NIR lasers on T-cell responses, we assessed the expression of cytokines in splenocytes from influenza-challenged mice. Both low and high doses of the 1258 nm handheld lasers significantly increased influenza-specific IFN-γ response compared to non-adjuvanted controls (Figure 5g, low dose: $P = 0.0024$; high dose: $P = 0.0125$). The handheld 1061 nm and 1301 nm (at low dose) as well as CW 1064 nm DPSSL induced modest increases with no significant difference. The 1061 nm and high dose 1258 nm handheld lasers also significantly increased influenza-specific IL-4 response compared to non-adjuvanted controls (Figure 5h, 1061 nm, $P = 0.0103$; 1258 nm high dose, $P = 0.0066$). These results show that the handheld NIR laser treatment significantly increases systemic immune responses to intradermal influenza vaccination and produces a mixed T_H1-T_H2 immune response without inducing an IgE response, which is equivalent to CW 1064 nm DPSSL [15].

The effect of the handheld NIR laser adjuvant on protective immunity

To investigate the effect of the handheld lasers on protective immunity, mice were challenged with homologous influenza virus, and monitored for body weight and survival time. Although there were no statistically significant differences among survival curves, the handheld 1061 nm, 1258 nm (both high and low doses) and 1301 nm low dose as well as 1064 nm DPSSL group showed a 20–25% lower mortality than the non-adjuvanted group (Figure 6a), which is consistent with our previous results [15]. Mice treated with the handheld 1061 nm, 1258 nm (both high and low doses) and 1301 nm low dose lost on average only 13–15% of their initial body weight compared to the 1301 nm low dose, 1064 nm DPSSL, no adjuvant control, and alum-adjuvanted groups, which incurred about 20% loss of the initial body weight at 6–7 days (Figure 6b).

Consistently, the HAI geometric mean titers (GMTs) measured on day 28 in the handheld 1061 nm (28.28, 95%CI, 18.99–42.13), 1258 nm (low dose: 40.0, 95%CI, 21.77–73.51, high dose: 28.28, 95%CI, 15.39–51.98) and 1301 nm low dose (40.0, 95%CI, 40.0–40.0) were higher than in the non-adjuvanted (11.34, 95%CI, 7.18–17.92), intramuscular route (11.49, 95%CI, 4.48–29.49), or Alum-adjuvanted group (10.91, 95%CI, 4.97–23.93) (Figure 6c). Post challenge, the HAI GMTs in the handheld 1061 nm (50.40, 95%CI, 27.83–91.27), 1258 nm (low: 60.63, 95%CI, 37.84–97.14, high: 28.28, 95%CI, 15.39–51.98) and 1301 nm low dose (40.0, 95%CI, 21.77–73.51) were similarly higher than in non-adjuvanted (17.63, 95%CI, 7.70–40.36), intramuscular route (8.71, 95%CI, 1.87–40.59), or Alum-adjuvanted group (16.82, 95%CI, 5.57– 50.83) (Figure 6d), although the differences were not statistically significant. These data suggest that the handheld NIR lasers combined with

intradermal influenza vaccination are capable of conferring protection against lethal viral challenge.

Discussion

In this study, we have established for the first time that a small, low-cost, handheld near-infrared (NIR) laser device using a semiconductor laser diode can replicate the adjuvant effect of a large DPSSL system. The NIR laser parameters of 1000–1300 nm can be readily translated into a clinically useful product that could be produced using low-power diodes that are 10–100 times less expensive than high-frequency, ultrashort duration pulsed lasers. Compared to other proposed laser adjuvant devices, which are inherently more expensive (e.g., P.L.E.A.S.E. type device [20, 21], the economics, simplicity and potential for compactness of a semiconductor diode-based laser make it a practical approach for large-scale clinical applications such as a prophylactic seasonal influenza vaccine. Specialized technical support is not needed for operation, and it can be programmed through a desktop or tablet computer to produce the desired parameters and record exposures and doses used.

We tested new NIR wavelengths including 1258 and 1301 nm and showed that these have equal or superior efficacy in augmenting intradermal vaccination at about half the power and dose of the 1061 nm laser. Use of these wavelengths has a number of inherent advantages over the use of the 1061–1064 nm wavelength. First, the variability of light absorption based on melanin pigment in the 1258–1301 range is almost negligible [22, 23], suggesting these devices would have a more uniform effect across skin colors. Second, as the power levels needed to augment immune responses for both of the wavelengths are significantly lower compared to that of 1061 nm, diode size could be reduced even further with a concomitant reduction in production cost. Thus far, 1258 nm appears to be the most effective wavelength with its ability to augment both humoral and cell-mediated immune responses. Further optimization of laser parameters of the handheld NIR laser adjuvant system is warranted for both practical and economic reasons for use in human vaccination.

Introducing traditional adjuvants into the skin causes inflammatory responses that last for weeks [9]. In contrast, the current study showed that the handheld lasers are capable of adjuvanting vaccine without inducing inflammation or damage to the skin tissue. The handheld NIR laser may therefore offer a feasible and economical option for use with an intradermal influenza vaccine for dose sparing. Anticipating of a continued logistical challenge in mass-vaccination programs against influenza, especially in resource-poor countries [24, 25], the handheld NIR laser adjuvant system opens a path for the development of vaccination with small antigen dose alternative to the standard intramuscular or subcutaneous influenza vaccination.

In summary, we have successfully developed low-cost, portable, programmable, handheld laser systems at NIR wavelength, which are capable of producing beam parameters equivalent to larger and more expensive DPSSL systems, and of inducing an adjuvant effect in an established murine vaccination system. The handheld laser systems establish the feasibility of using the NIR laser adjuvant approach for mass-vaccination programs in a clinical setting and provide the basis for development of devices ready for use in the clinic.

Supplementary Material

Refer to Web version on PubMed Central for supplementary material.

Acknowledgments

We thank Madeline Penson (Massachusetts General Hospital) for her excellent technical assistance.

Funding: Research reported in this manuscript was supported by the National Institute of Allergy and Infectious Diseases of the National Institutes of Health under award number R41AI114012 (J.C.), R42AI114012 (D.B.), R01AI105131 (S.K.), Kanae Foundation for the Promotion of Medical Science (Y.K.), Mochida Memorial Foundation for Medical and Pharmaceutical Research (Y.K.), Uehara Memorial Foundation (Y.K.), Japan Foundation for Pediatric Research (Y.K.), and the VIC Innovation Fund (S.K.). The funders had no role in study design, data collection and analysis, decision to publish, or preparation of the manuscript.

References

1. Fehres CM, Garcia-Vallejo JJ, Unger WW, van Kooyk Y. Skin-resident antigen-presenting cells: instruction manual for vaccine development. Front Immunol. 2013; 4:157. [PubMed: 23801994]
2. Sticchi L, Alberti M, Alicino C, Crovari P. The intradermal vaccination: past experiences and current perspectives. J Prev Med Hyg. 2010; 51:7–14. [PubMed: 20853670]
3. Combadiere B, Liard C. Transcutaneous and intradermal vaccination. Hum Vaccin. 2011; 7:811–27. [PubMed: 21817854]
4. Kim YC, Jarrahian C, Zehrung D, Mitragotri S, Prausnitz MR. Delivery systems for intradermal vaccination. Curr Top Microbiol Immunol. 2012; 351:77–112. [PubMed: 21472533]
5. Zehrung D, Jarrahian C, Wales A. Intradermal delivery for vaccine dose sparing: overview of current issues. Vaccine. 2013; 31:3392–5. [PubMed: 23176978]
6. Lambert PH, Laurent PE. Intradermal vaccine delivery: will new delivery systems transform vaccine administration? Vaccine. 2008; 26:3197–208. [PubMed: 18486285]
7. Nicolas JF, Guy B. Intradermal, epidermal and transcutaneous vaccination: from immunology to clinical practice. Expert Rev Vaccines. 2008; 7:1201–14. [PubMed: 18844594]
8. Hickling JK, Jones KR, Friede M, Zehrung D, Chen D, Kristensen D. Intradermal delivery of vaccines: potential benefits and current challenges. Bulletin of the World Health Organization. 2011; 89:221–6. [PubMed: 21379418]
9. Vitoriano-Souza J, Moreira N, Teixeira-Carvalho A, Carneiro CM, Siqueira FA, Vieira PM, et al. Cell recruitment and cytokines in skin mice sensitized with the vaccine adjuvants: saponin, incomplete Freund's adjuvant, and monophosphoryl lipid A. PLoS ONE. 2012; 7:e40745. [PubMed: 22829882]
10. Chen X, Pravetoni M, Bhayana B, Pentel PR, Wu MX. High immunogenicity of nicotine vaccines obtained by intradermal delivery with safe adjuvants. Vaccine. 2012; 31:159–64. [PubMed: 23123021]
11. Kashiwagi S, Brauns T, Poznansky MC. Classification of Laser Vaccine Adjuvants. J Vaccines Vaccin. 2016; 7
12. Kashiwagi S, Brauns T, Gelfand J, Poznansky MC. Laser vaccine adjuvants. History, progress, and potential. Hum Vaccin Immunother. 2014; 10:1892–907. [PubMed: 25424797]
13. Onikienko SB, Zemlyanoy AB, Margulis BA, Guzhova IV, Varlashova MB, Gornostaev VS, et al. Diagnostics and correction of the metabolic and immune disorders. Interactions of bacterial endotoxins and lipophilic xenobiotics with receptors associated with innate immunity. Donosologiya (St Petersburg). 2007; 1:32–54.
14. Chen X, Kim P, Farinelli B, Doukas A, Yun SH, Gelfand JA, et al. A novel laser vaccine adjuvant increases the motility of antigen presenting cells. PLoS ONE. 2010; 5:e13776. [PubMed: 21048884]
15. Kashiwagi S, Yuan J, Forbes B, Hibert ML, Lee EL, Whicher L, et al. Near-infrared laser adjuvant for influenza vaccine. PLoS One. 2013; 8:e82899. [PubMed: 24349390]

16. Callahan JJ, McIntyre E, Rafferty C, Yanushefski L, Bean DM. Low-cost/high-efficiency lasers for medical applications in the 14XX-nm regime. Proc SPIE. 2011; 7883:78830O.
17. Frey A, Di Canzio J, Zurakowski D. A statistically defined endpoint titer determination method for immunoassays. J Immunol Methods. 1998; 221:35–41. [PubMed: 9894896]
18. Gupta RK, Rost BE, Relyveld E, Siber GR. Adjuvant properties of aluminum and calcium compounds. Pharmaceutical biotechnology. 1995; 6:229–48. [PubMed: 7551219]
19. Coffman RL, Sher A, Seder RA. Vaccine adjuvants: putting innate immunity to work. Immunity. 2010; 33:492–503. [PubMed: 21029960]
20. Bloom BS, Brauer JA, Geronemus RG. Ablative fractional resurfacing in topical drug delivery: an update and outlook. Dermatologic surgery: official publication for American Society for Dermatologic Surgery [et al]. 2013; 39:839–48.
21. Sklar LR, Burnett CT, Waibel JS, Moy RL, Ozog DM. Laser assisted drug delivery: a review of an evolving technology. Lasers Surg Med. 2014; 46:249–62. [PubMed: 24664987]
22. Sliney DH, Palmisano WA. The evaluation of laser hazards. Am Ind Hyg Assoc J. 1968; 29:425–31. [PubMed: 5727078]
23. Boulnois J-L. Photophysical processes in recent medical laser developments: A review. Lasers in Medical Science. 1986; 1:47–66.
24. Hessel L, European Vaccine Manufacturers Influenza Working G. Pandemic influenza vaccines: meeting the supply, distribution and deployment challenges. Influenza Other Respir Viruses. 2009; 3:165–70. [PubMed: 19627373]
25. Partridge J, Kieny MP. Global production capacity of seasonal influenza vaccine in 2011. Vaccine. 2013; 31:728–31. [PubMed: 23149268]

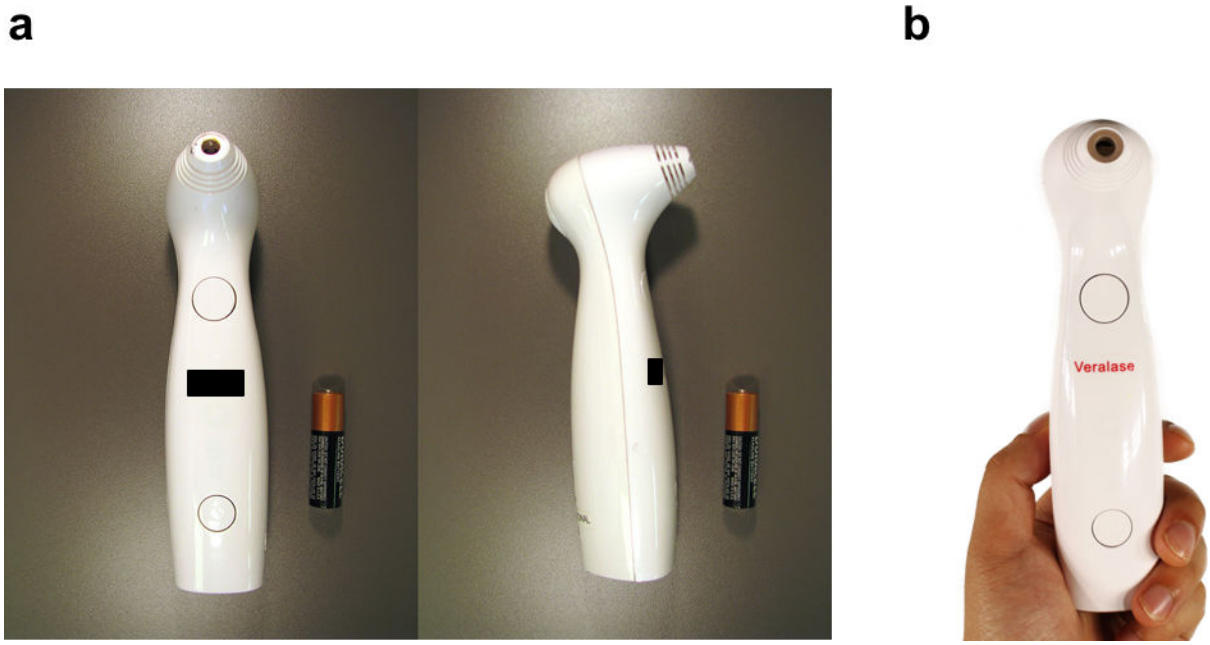

Figure 1. Final assembly of handheld laser system

(a), The housing was approximately 150 mm in length and contained the laser engine, control board, rechargeable battery, USB interface and remote operation connection. The laser emits through the 6 mm diameter hole located at the top of the device. (b), The handheld is designed to fit with a hand with the top “fire” or “trigger” button located in the thumb position.

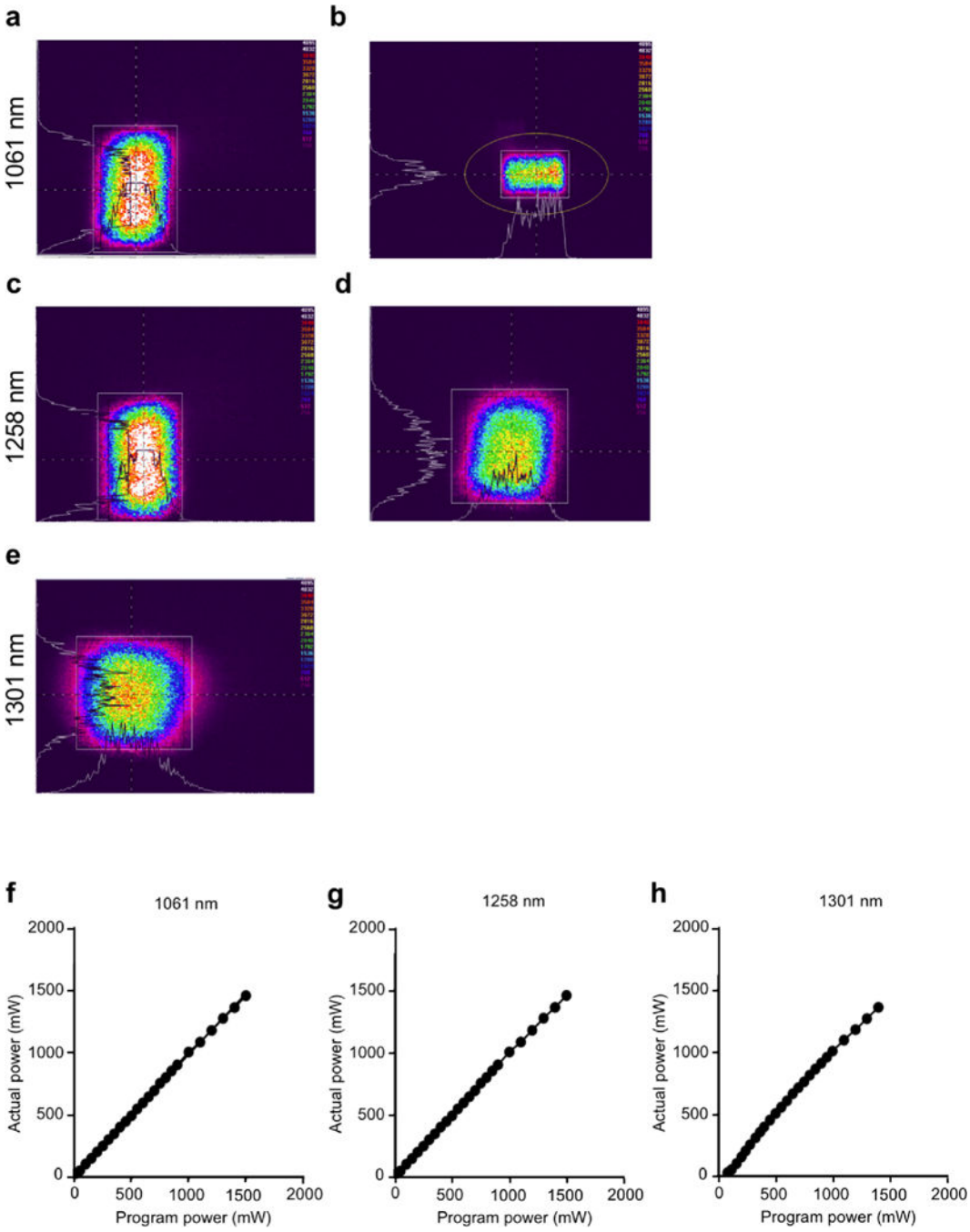

Figure 2. The beam profile of the handheld laser

The beam profiles revealed with an IR camera for the 1061 nm (a), uncorrected (b), corrected with nosecone, 1258 nm (c), uncorrected and (d), c corrected with nosecone and 1301 nm (e), uncorrected images. The 1301 nm laser produced a square spot from the onset, hence no nosecone was needed for this testing. The colors indicate the intensity of the energy emitted from the laser. The intensity level is arbitrary. The white lines on the horizontal and vertical axis are the intensity profiles across the center of each spot. The white box and orange circle are used by the imaging software for identifying areas of

interest. (f–h), input power was plotted against output power. Average output powers were determined using a power meter. (f), 1061 nm, (g), 1258 nm and (h), 1301 nm wavelength laser diodes where (actual power) =0.9842 (Program power) + 11.04 (linear regression, R^2=0.9998), (actual power) = 0.9775 (Program power) + 9.238 (linear regression, R^2=0.9996), (actual power) = 1.027 (Program power) – 28.64 (linear regression, R^2=0.9964). The actual power delivered is equal to the programmed to within ± 5% which enables the researcher to consistently and repeatedly obtain and use the parameters without using a calibration factor. Data are representative of three independent experiments.

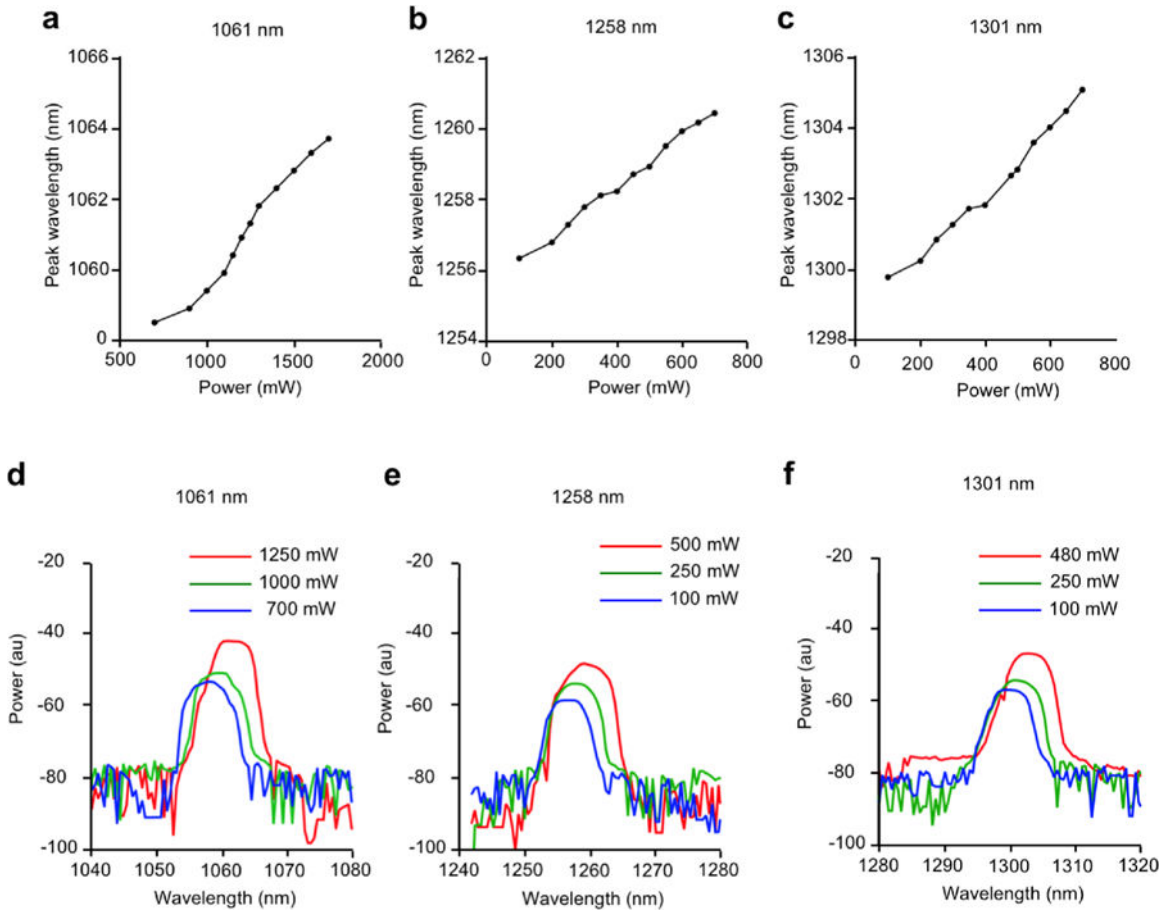

Figure 3. Peak wavelength vs. programmed power of the handheld devices

The wavelength was measured in 0.2 nm steps by an optical spectrum analyzer. (a–c), Peak wavelength for (a), 1061 nm, (b), 1258 nm and (c), 1301 nm device in a range of input power. (d–f), wavelength profile at non-tissue damaging powers for (d) 1061 nm, (e), 1258 nm and (f), 1301 nm device. Data are representative of three independent experiments.

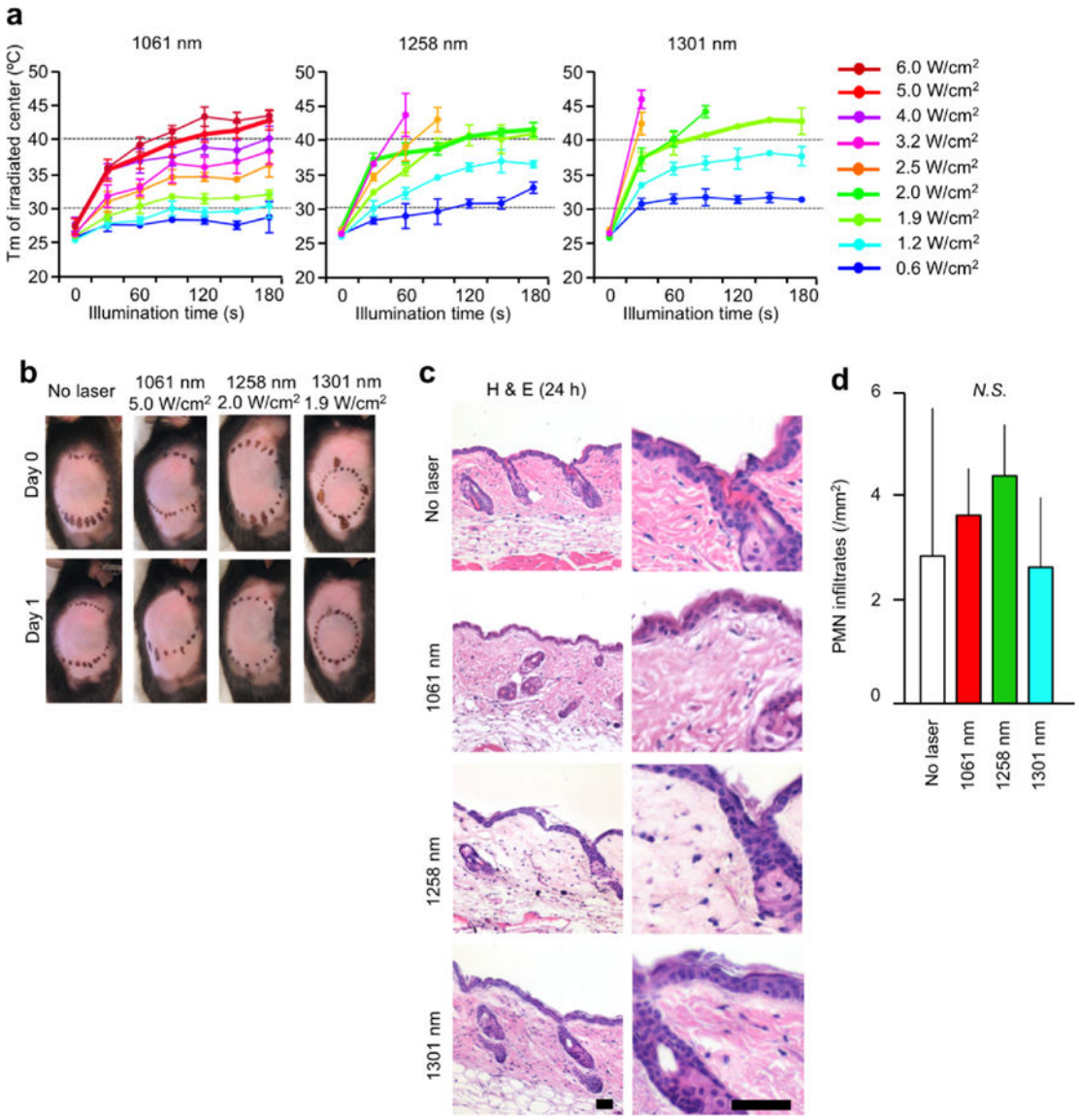

Figure 4. Effect of the handheld near-infrared (NIR) laser adjuvant on skin tissue

(a), Dose-temperature responses of the handheld NIR lasers in mouse skin. n=1–10 for each group. NIR, near-infrared; Tm, maximal skin surface temperature. Error bars show means ± s.e.m. (b), Images of the back of mice for visual inspection at 0 and 24 hours after the handheld NIR laser treatment. Representative images for each group are presented. (c), Microscopic assessment of skin damage and inflammatory infiltration after laser treatment. Representative time-course images of hematoxylin-eosin-stained skin tissue are presented. The bar indicates 50 μm. (d), Quantification of polymorphonuclear leukocytes (PMN) after the hand held NIR laser treatment. (b–d), n = 2–3 for each group. Note that there was no significant difference in PMN counts among control and experimental groups. Results are pooled from two independent experiments.

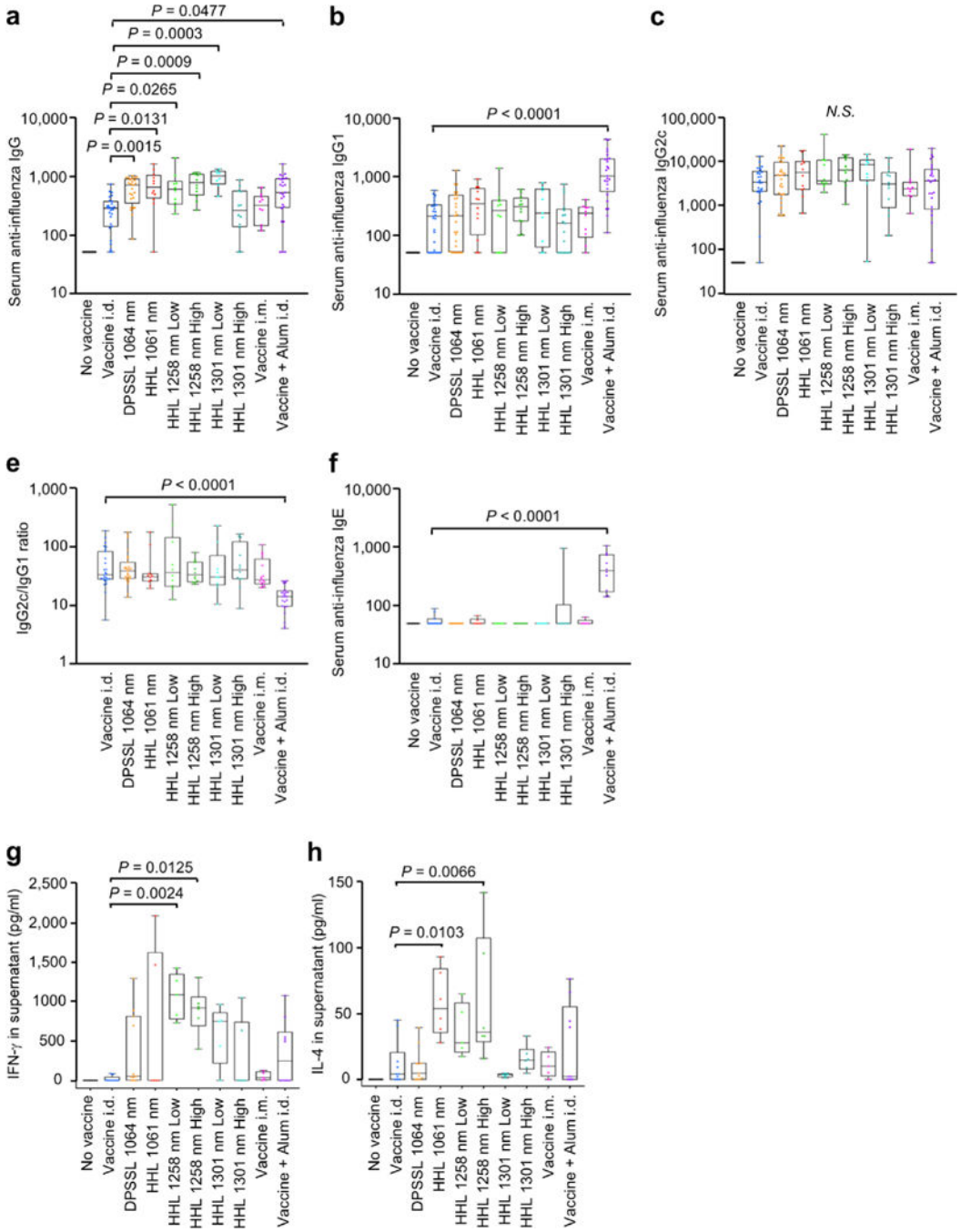

Figure 5. Effect of the handheld NIR laser adjuvant on anti-influenza immune responses

(a–c), Influenza-specific IgG subclass titers in post-challenge (4 days after challenge). Mice were vaccinated with 1 μg of inactivated influenza virus (A/PR/8/34) with or without laser illumination or the licensed chemical adjuvant (alum) and challenged intranasally with live homologous virus 4 weeks after vaccination. Titer of influenza-specific serum IgG subclass was determined by ELISA. Plates were coated with inactivated influenza virus. One-way ANOVA followed by the Tukey's honestly significant difference (HSD) tests. (a) IgG, (b) IgG1 and (c) IgG2c titers. (e) IgG2c/IgG1 ratio. (f) IgE titers. Experimental and control

groups: (a–e) n= 25, 27, 27, 12, 10, 12, 10, 12, 10, 25, (f) n= 10, 11, 11, 6, 5, 6, 5, 6, 5, 10 for no vaccine, vaccine i.d., vaccine i.d. + DPSSL 1064 nm, vaccine i.d. + HHL 1064 nm, vaccine i.d. + HHL 1270 nm low dose, vaccine i.d. + HHL 1270 nm high dose, vaccine i.d. + HHL 1310 nm low dose, vaccine i.d. + HHL 1310 nm high dose, vaccine i.m., and vaccine + Alum i.d. vaccine groups, respectively. (a–f), Results are pooled from four independent experiments. (g–h), Systemic T-cell responses were measured 4 days after challenge by re-stimulating 1×10^6 splenocytes with a nucleoprotein (NP) major histocompatibility class-II complex (MHC) or class-I influenza-specific peptide. Levels of (g) IFN-γ (h) IL-4 in splenocyte culture supernatants are shown. Oneway ANOVA followed by the Tukey's honestly significant difference (HSD) tests. Experimental and control groups: (g–h) n= 10, 11, 11, 6, 5, 6, 5, 6, 5, 10 for no vaccine, vaccine i.d., vaccine i.d. + DPSSL 1064 nm, vaccine i.d. + HHL 1064 nm, vaccine i.d. + HHL 1270 nm low dose, vaccine i.d. + HHL 1270 nm high dose, vaccine i.d. + HHL 1310 nm low dose, vaccine i.d. + HHL 1310 nm high dose, vaccine i.m., and vaccine + Alum i.d. vaccine groups, respectively. (g–h), Results are pooled from two independent experiments.

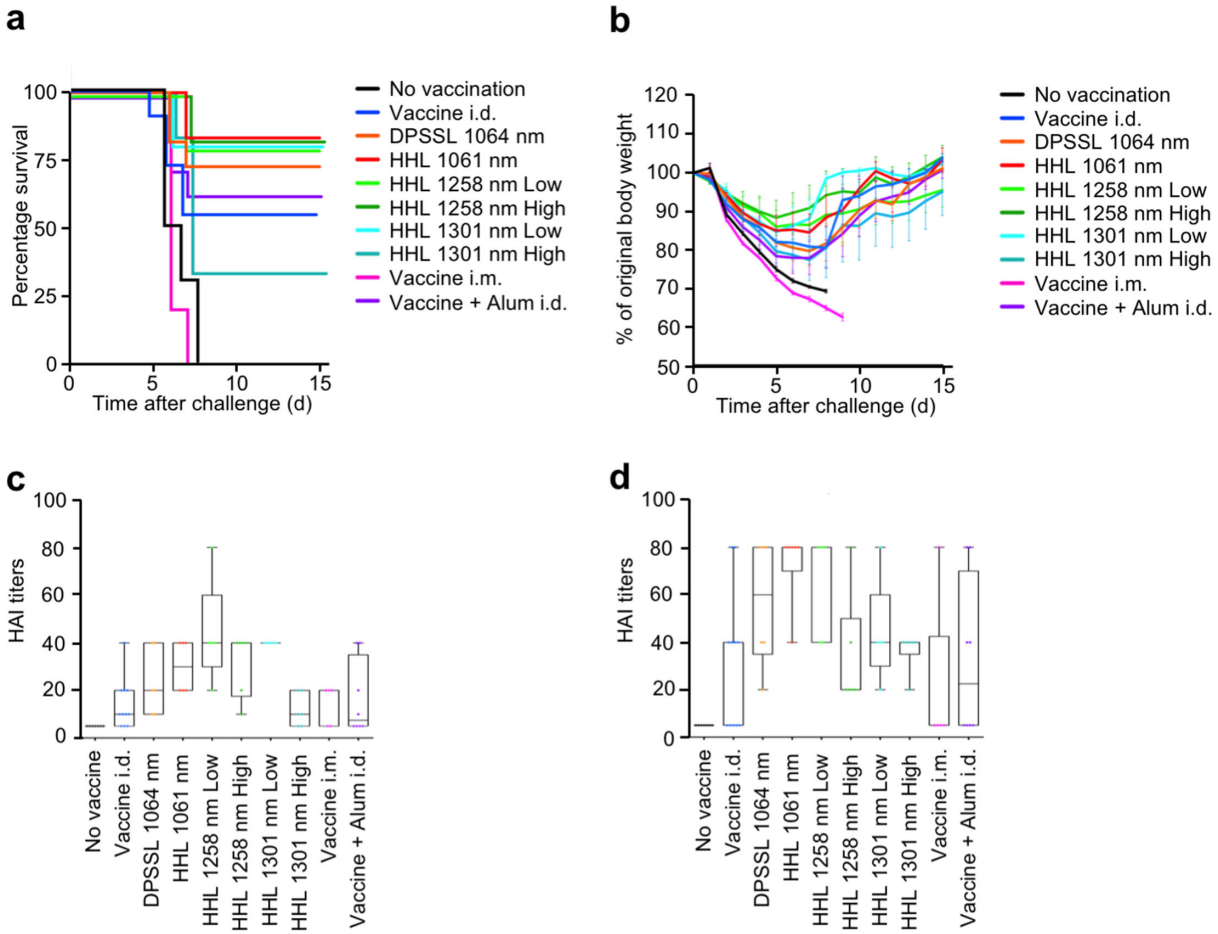

Figure 6. Effect of the handheld NIR laser adjuvant on protective immunity

(a), Kaplan-Meier survival plots of influenza-vaccinated mice for 15 days following lethal challenge. (b), Body weights were monitored daily for 15 days. The arithmetic mean ± s.e.m. of percent of original body weight for each experimental group at each time point are displayed. (c–d), HAI titers (c) in pre-challenge (4 weeks after vaccination) and (d) post-challenge (4 days after challenge) serum. Experimental and control groups: (a–b) n=9, 16, 16, 16, 16, 16, 16, 16, 10, 16, (c–d) n=7, 11, 6, 6, 5, 6, 5, 6, 5, 8 for no vaccine, vaccine i.d., vaccine i.d. + DPSSL 1064 nm, vaccine i.d. + HHL 1064 nm, vaccine i.d. + HHL 1270 nm low dose, vaccine i.d. + HHL 1270 nm high dose, vaccine i.d. + HHL 1310 nm low dose, vaccine i.d. + HHL 1310 nm high dose, vaccine i.m., and vaccine + Alum i.d. vaccine groups, respectively. Results are pooled from four independent experiments.